ISSN 1330-3651 (Print), ISSN 1848-6339 (Online)
https://doi.org/10.17559/TV-20250129002304
Original scientific paper

Dual-Band Rectenna for RF Energy Harvesting in GSM 900 and GSM 1800 Bands for IoT Applications

V. GANESH*, H. MANGALAM

Abstract: This paper presents a dual-band rectenna designed for RF energy harvesting in GSM 900 and GSM 1800 frequency bands, targeting the sustainable powering of low-power devices such as wireless sensor nodes, wearable electronics, and IoT sensors. The antenna features a double-sided printed dipole, double-sided parallel strip line, microstrip feed line, reflector, and parasitic dipole elements. The fabricated antenna covers the impedance bandwidth of both target frequency bands, with half-power beam widths of 150° at 0.945 GHz and 230° at 1.84 GHz based on measured H-plane radiation patterns. A stacked two-branch rectifier circuit is developed to rectify signals within the desired bands, incorporating Schottky diodes, matching networks, a power divider, and a DC-pass filter. Single-stub and double-stub matching networks optimized with high-impedance transmission lines enhance the bandwidths for GSM 900 and GSM 1800 bands, respectively. The rectifier achieves a maximum efficiency of 44.8% and 46.5% at -5 dBm for 920 MHz and 1766 MHz, respectively. The fabricated rectenna delivers a maximum DC output voltage of 673 mV at a 4.7 kΩ load in outdoor conditions, demonstrating its potential for powering low-power devices in sustainable IoT and energy-harvesting applications.

Keywords: dual-band antenna; IoT energy solutions; rectenna; RF energy harvesting; wireless sensor nodes

1 INTRODUCTION

Ambient RF energy harvesting technology has recently gained popularity due to the increasing demand for Internet of Things (IoT) devices and wearable technologies. The frequent replacement of batteries poses a significant challenge for many portable low power electronic devices and contributes to environmental pollution due to the disposal of used batteries. This has created a demand for battery-free electronic devices, a need addressed by Radio Frequency Energy Harvesting (RFEH) technology which enables wireless powering of devices. The key component of this technology is the rectenna, which integrates an antenna and a rectifier to capture and convert RF energy into DC power. The RF power density is typically very low in an ambient environment. Additionally, the Power Conversion Efficiency (PCE) of the rectifier is influenced by the level of received RF power. To maximize the harvested power, one effective approach is the use of multi-band or wideband rectenna.

The key properties required for a receiving antenna in RF energy harvesting are omnidirectional radiation pattern, multiband or wideband operation, and the ability to capture RF energy from random polarizations. Current state-of-the-art antenna designs for energy harvesting include multiband antennas, low-profile antennas, array antennas polarization-sensitive antennas, and various fabrication techniques [1, 2]. A simple half-wavelength dipole antenna operating at 915 MHz is folded to reduce its size, and a slot is introduced at the center of the antenna to create a second resonance frequency at 2.45 GHz. The measured antenna gains were 1.87 dBi at 915 MHz and 4.18 dBi at 2.45 GHz [4]. A Yagi dipole antenna was designed on an FR4 substrate to capture GSM 1800 and Wi-Fi signals. The antenna exhibits wideband characteristics, operating from 1.54 GHz to 3.22 GHz, with a gain ranging from 7.5 to 10.5 dBi [5]. A slotted bow-tie antenna with varying numbers of slits was designed for energy harvesting of multiband signals, offering a wider bandwidth, high gain, and a low front-to-back ratio [8]. A 1×4 quasi-Yagi array was designed for energy harvesting in the GSM-1800 and UMTS-2100 bands, providing a gain range of 9.9 to 13.3 dBi at 1.85 GHz and 10.9 to 13.3 dBi at 2.15 GHz [9]. A planar monopole antenna was designed to capture signals in the 900 MHz frequency band. Instead of using a quarter-wavelength design for the monopole antenna, the lengths of both the antenna and the feeder were adjusted to ensure that the antenna impedance is purely resistive and properly matched to the rectifier [10]. In references [26-28], compact microstrip antennas are discussed for wireless applications at the ISM, Wi-Fi, and WLAN bands.

The antennas mentioned above were proposed for energy harvesting, with key parameters including omnidirectional radiation pattern, gain, bandwidth, size and polarization. In this work, a dual-band antenna is comprising a double-sided printed dipole antenna with a parasitic dipole. The antenna's impedance bandwidth is enhanced using a double-sided parallel strip line, and the second band is achieved by placing a parasitic dipole close to the driven dipole. The measured radiation properties of the antenna are well-suited for ambient RF energy harvesting in both bands.

The architecture of multi-band rectifier is single branch multi-band rectifier circuit [9, 17, 19] and multiple branches of single-band rectifier circuit in each branch [8]. The single branch multi-band rectifier topology is not guaranteed to cover the entire band of operating frequencies [20]. But, the multiple branch rectifier topology enhances the rectification of entire band of operation whereas the size of the rectifier is increased when compared to the single branch multi-band rectifier [17, 20]. At low power level, series mounted diode provides more rectification efficiency [22]. A single rectifier for each frequency band enhances the PCE [8]. Compared to wideband rectenna, interference due to other bands is eliminated in the multi-band rectenna [16].

In [4], a dual-band compact rectifier was designed with a single-stage matching network comprising three inductors and a radial stub. The measured reflection coefficient is greater than –5 dB at 0.915 GHz and above –10 dB at 2.45 GHz. The reflection coefficient was analyzed for a single input RF power level. The PCE remains low for input power levels below –20 dBm. In [6], a single-stage matching network was designed using inductors and CPW. The PCE was measured from –15 dBm to 0 dBm, with the rectifier's performance being lower at 1.880 GHz compared to the 1.980 GHz frequency. In [9], a single-stage, two-section T-shaped microstrip transformer was used to achieve dual-band characteristics, thereby enhancing the bandwidth. An acceptable PCE was attained for ambient power levels below -5 dB in the GSM-1800 and UMTS-2100 bands. This improved performance was achieved with a size of 146 × 27 mm. In [17], a dual-band rectifier was designed for the 3.5 GHz 5G band and the 5.8 GHz Wi-Fi band for RFEH/MPT applications. A half-wave line was used to resonate the second band. A single-stage matching network was implemented with a quarter-wave line and a stub. The circuit showed better performance at 3.5 GHz compared to the second band, and the rectifier's operating power range spans from –3 dBm to 14.5 dBm, which is outside the typical ambient power levels. In [19], a single-stage stepped impedance matching network was incorporated into an efficient dual-band rectifier design for wireless energy harvesting. The uniform impedance single stub was replaced with a stepped impedance stub to enable dual-band operation at 0.915 GHz and 2.45 GHz. The design was evaluated with a fixed load resistance of 1.5 KΩ, and the reflection coefficient was measured at an RF power of 9 dBm. The PCE at an input power level of –20 dBm was very low for both frequencies. In [23], a dual-branch band pass filter was designed to maximize power transmission from the antenna to the rectifier, utilizing inductors and microstrip lines. The PCE and output DC voltage were analyzed over a range of input powers from –15 dBm to 15 dBm. The reported PCE was very low for input RF power levels below 0 dBm. In [24], a single-branch multi-stub impedance matching network was designed for the GSM-1800, UMTS-2100, and Wi-Fi bands. The design offers a total of 20 degrees of freedom, with the rectifier sized at 41 × 81 mm. A good PCE was achieved at low RF power levels ranging from –30 dBm to –10 dBm. To minimize insertion loss, a very low-loss substrate, RT/Duroid 5880, with a dielectric constant of 2.2 and a loss tangent of 0.0009, was used. In [25], a single-stage matching network was designed using a cross-shaped match stub and a T-shaped match stub to rectify the 2.45 GHz and 5.8 GHz signals. At the second resonance of 5.8 GHz, the efficiency is significantly lower compared to the first resonance at 2.45 GHz. The reflection coefficient was not analyzed, and the results were presented for a fixed load of 2 KΩ. The challenges observed in these studies on dual-band rectifier circuits emphasizes a trade-off between performance, size, and operating range (frequency, input power levels, and load resistance) as well as the variation in PCE across the two frequency bands. The rectifier circuit designed in this work, featuring a matching network, aims to address these limitations, specifically for energy harvesting in the GSM 900 and GSM 1800 bands. This is achieved by transforming the variable diode input impedance into a nearly constant impedance using a high-impedance line of appropriate electrical length, across varying ambient power levels, operating frequencies, and load resistances ranging from 3 KΩ to 10 KΩ.

2 ANTENNA

Compared to the microstrip patch antenna configuration, the double-sided printed dipole antenna with parasitic elements offers advantages such as increased bandwidth, multi-frequency resonance, and reduced substrate area requirements [12]. The bandwidth of the double-sided printed dipole antenna is improved using the Double-Sided Parallel Strip (DSPS) line. The DSPS line is a balanced transmission line comprising two parallel strip lines separated by a dielectric layer. The frequency-independent out-of-phase characteristic of the DSPS line makes it suitable for use in balanced circuits to enhance performance [14]. The parasitic element is placed close to the driven element to achieve the dual band operation [12]. Based on the double sided printed diploe antenna and parasitic dipole reported by the previous researches [12, 13], in this work a dual band printed diploe antenna with parasitic diploe is designed to harvest energy in the GSM900 and GSM1800 bands with wider beamwidth and moderate gain.

2.1 Antenna Design

The layout of the antenna is shown in Fig. 1.

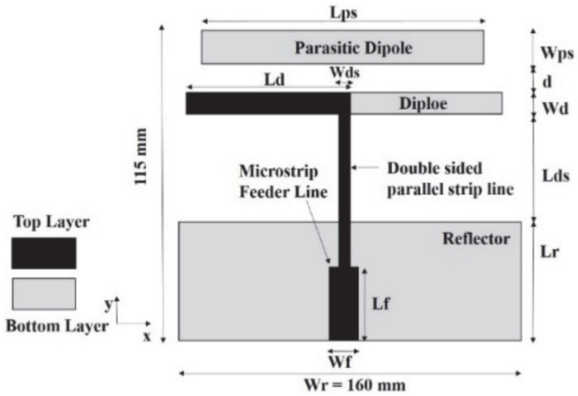

Figure 1 Layout of the printed dipole antenna with parasitic dipole

The antenna is designed on a 0.76 mm thick Roggers RT Duroid 3203 substrate with dielectric constant 3.02 and loss tangent of 0.0016. One arm of the driven dipole, one of the lines of parallel strip line and a microstrip feeder line are printed on one side of the substrate. The other side of the substrate consists of the second arm of the driven dipole printed in opposite direction, along with the other line of parallel strip line, a truncated ground plane and a parasitic dipole. The balanced antenna impedance is matched to 50 Ω unbalanced microstrip feeder line using a quarter wave impedance transformer of DSPS line. The truncated ground plane acts as a reflector [11-13]. The initial dimensions of driven dipole and parasitic dipole are chosen as half wavelength ($\lambda_g/2$) at the center frequency, then the final dimensions are optimized for the bandwidth of GSM 900 and 1800 bands using 3D EM simulator Ansys HFSS software. The parametric study of design parameters d, W_{ps}, L_{ds}, W_{ds} and L_r are carried out in the simulation and the reflection coefficient values are shown as in Fig. 2. When the parasitic element is placed so close to the dipole in the space *d*, it increases the coupling but creates an impedance mismatch. The better impedance matching is achieved for an optimum value of d at 2.5 mm as shown in Fig. 2a. The width of the parasitic dipole (W_{ps}) is related to the quality factor of the resonance. The optimum value of W_{ps} is obtained at 8.5 mm as shown in Fig. 2b. The impedance bandwidth of the antenna is achieved by the DSPS line which is placed between the reflector and driven element. The optimum length (L_{ds}) and width (W_{ds}) are 50 mm and 1.6 mm respectively, as shown in Fig. 2c and 2d. The length of the reflector (L_r) also controls the impedance bandwidth, with the optimal being 50 mm, as shown in Fig. 2e. The final optimized dimensions of the antenna are presented in Tab. 1.

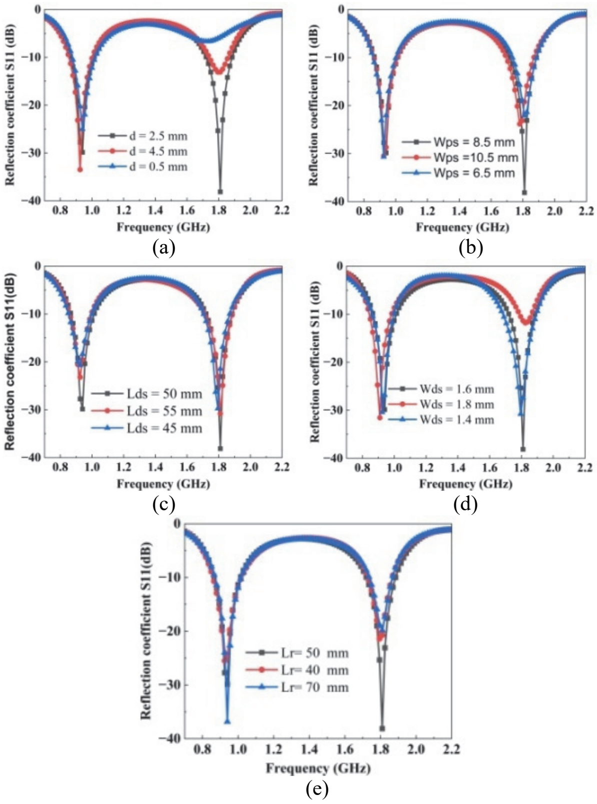

Figure 2 Simulated reflection coefficient of the antenna with different design parameters: (a) d; (b) W_{ps}; (c) L_{ds}; (d) W_{ds}; (e) L_r

Table 1 Optimized antenna design parameters

Parameter	Dimension mm
Length of the dipole of one arm (L_d)	72
Width of the dipole (W_d)	4
Length of the parasitic strip (L_{ps})	64
Width of the parasite strip (W_{ps})	8.5
Spacing between driven element and parasitic strip (d)	2.5
Length of double sided printed line (L_{ds})	50
Width of double sided printed line (W_{ds})	1.6
Length of the microstrip feeder line (L_f)	30
Width of the microstrip feeder line (W_f)	1.9
Length of the reflector (L_r)	50
Width of the reflector (W_r)	160

2.2 Performance of the Designed Antenna

To validate the antenna design, the antenna was fabricated, and photographs of the fabricated antenna are shown in Fig. 3. The antenna parameters, the reflection coefficient and radiation pattern, were measured using a Network Analyzer and in an Anechoic Chamber, as depicted in Figs. 4a and 4b, respectively.

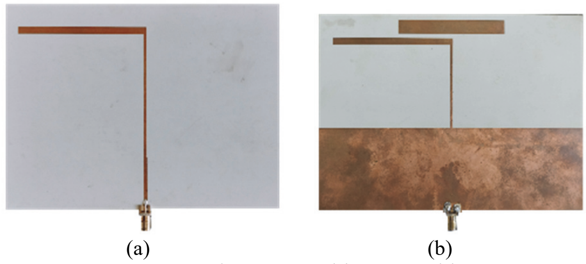

Figure 3 Photographs of the antenna. (a) Top view; (b) Bottom view

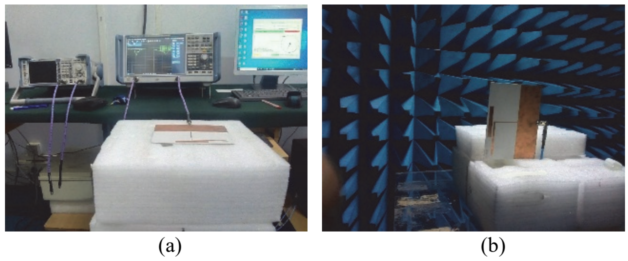

Figure 4 Measurement setup for measuring antenna parameters: (a) Reflection coefficient; (b) Radiation pattern

The simulated and measured reflection coefficients S11 in dB and peak gain are shown in Fig. 5. The measured –10 dB impedance bandwidths are 132 MHz [872-1004 MHz] and 168 MHz [1712-1880 MHz] which covers the GSM 900 and 1800 bands. The measured gain ranges from 3 dBi to 4.8 dBi in the GSM 900 band and from 2.5 dBi to 3.2 dBi in the GSM 1800 band. The measured maximum gain of 4.8 dBi and 3.2 dBi is achieved at 956 MHz and 1796 MHz respectively. The simulated and measured E-plane and H-plane patterns are shown in Fig. 6. From the measurement of radiation pattern, it is observed that the half-power beamwidth (HPBW) in H-plane is about 150° and 230° at 0.945 GHz and 1.84 GHz respectively. The cross polarization levels in both the E- plane and H plane are low.

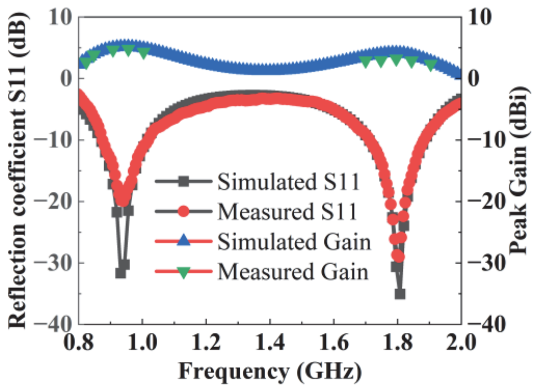

Figure 5 Reflection coefficient and peak gain of the antenna

The reflector is positioned approximately a quarter wavelength away from the driven element at the GSM 900 band, resulting in higher gain and a lesser beamwidth for the GSM 900 band compared to the GSM 1800 band. The measured results closely match the simulated results for the designed antenna, and its observed radiation properties are suitable for ambient RF energy harvesting in the GSM 900 and 1800 bands.

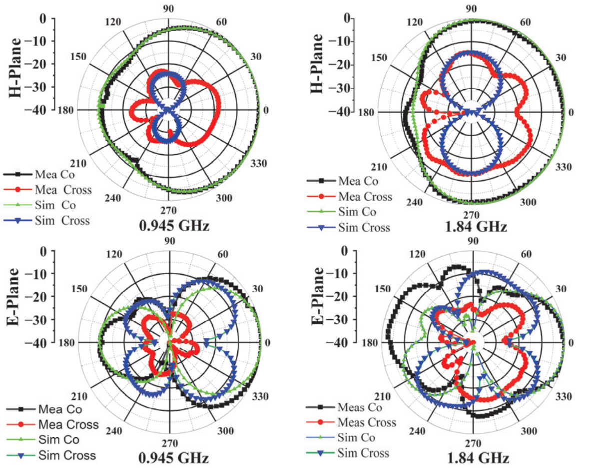

Figure 6 Simulated and measured radiation pattern

3 RECTIFIER

The rectifier is used to convert the received RF energy into DC voltage and current. Typically, a RF rectifier provides high rectification efficiency for a specific input power, central frequency, and load impedance. However, when operating outside these defined limits, the conversion efficiency of the rectifier significantly decreases [24]. This limitation is mainly due to impedance mismatch between the antenna and the rectifier. Due to the non-linearity of the diode, its input impedance changes with variations in input power level, frequency, and load. Therefore, at low RF power levels, designing an efficient matching network becomes a crucial aspect of rectifier design. The objective of this research is to design a rectifier with a matching circuit to mitigate these limitations to some extent, specifically for energy harvesting in the GSM 900 and GSM 1800 bands.

3.1 Rectifier Design

The maximum power that the antenna can receive from the ambient environment is very low, typically ranging from –30 dBm to –5 dBm [21]. Based on the power levels, three rectifier topologies are basically used namely: Series mounted diode for low power levels (below 0 dBm, 50 % PCE); Shunt mounted diode for medium power levels (0 to 20 dBm, 70%); and Bridge rectifier for higher power levels (greater than 20 dBm), 78% [23]. The multiband single-branch rectifier topology is unable to cover the intended broad frequency range, whereas the multiband parallel-branch rectifier stacked topology effectively covers the required frequency band of interest. Hence, a stacked topology with series configuration half wave rectifier for two GSM bands is proposed comprising two diodes, matching networks, T- junction power divider network and a DC-pass filter. The schematic of the proposed rectifier is shown in Fig. 7. The LSSP and Harmonic balance analysis setup in Advanced Design System (ADS) software is used to analyse the results of schematic and layout level simulation. A Schottky diode, Avago HSMS 2850 (Series resistance R_s = 25 Ω, Threshold voltage V_{th} = 150 mV, Junction capacitance C_{jo} = 0.18 pF, Breakdown voltage = 3.8 V) is selected for rectifying low power RF signals, as it was specially designed and optimized for small signal applications. The diode input impedance (Z_d) values are determined for the circuit consisting of the rectifier, DC-pass filter, and load resistor at the lower, upper, and mid frequencies of the two bands, under maximum power transfer conditions, by complex conjugating the load impedance in the schematic. This work focuses on energy harvesting from the GSM 900 and 1800 bands in the ambient environment. So an initial input power level of –15 dBm is used for determining the diode's input impedance value.

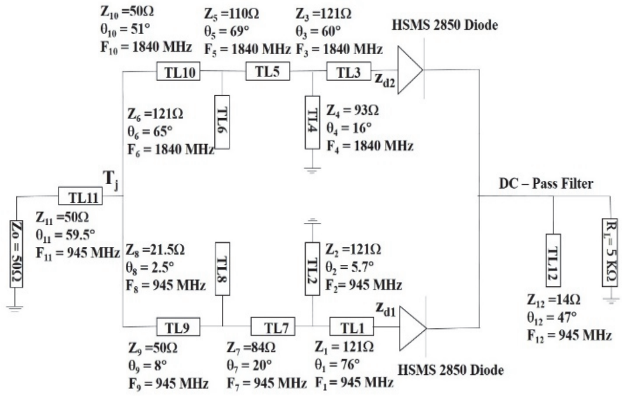

Figure 7 Schematic of the proposed rectifeir circuit

The transmission line-based matching network design principle is illustrated in Fig. 8. In this design, the lower branch of the impedance Z_{d1} is matched using a single stub technique with transmission lines TL1 and TL2 for the GSM 900 downlink frequency. High-impedance transmission lines TL1 and TL2 are employed to improve the bandwidth. The impedance at the output of TL2 is transformed closer to the characteristic impedance (Zo) using a T-junction power divider, which further broadens the impedance bandwidth. The power divider network comprises short high-impedance line TL7, a low-impedance open-circuit line TL8, and 50 Ω lines TL9, TL10, and TL11. The susceptance in the upper branch for the GSM 900 band is cancelled by adjusting the dimensions of TL7, TL8, TL9, and TL10. The impedance at various points in the circuit is shown in Fig. 9a when both branches operate simultaneously at 0.945 GHz. In the upper branch, a double-stub matching technique is used for the GSM 1800 downlink frequency. The impedance of the upper branch, Z_{d2}, is brought within the r = 1 circle on the Smith chart using transmission lines TL3 and TL4. The impedance is then further transformed to the g = 1 circle with a section of transmission line TL5. An open-circuited line, TL6, is employed to cancel the susceptance generated at the output of TL5. Finally, the susceptance in the lower branch for the GSM 1800 band is cancelled by adjusting the dimensions of TL7, TL8, TL9, and TL10. When both branches operate simultaneously at 1.84 GHz, the impedance at different locations in the circuit is shown in Fig. 8b. The short circuited lines TL2 and TL4 also provide DC ground for the rectifier. The high-impedance lines TL1 along with their electrical length, transform the variable diode input impedance into a nearly constant impedance for power levels ranging from –30 dBm to 0 dBm at the downlink frequencies of GSM 900 band, with a 4.7 kΩ load resistor. Similarly the high impedance line TL3 is also transform diode input impedance into a nearly constant impedance at GSM 1800 down link frequencies. The impedance variation at the output section of TL1 and TL3 remains minimal for load values between 3 kΩ and 7.5 kΩ, within the same power range of –30 dBm to 0 dBm for the GSM 900 and 1800 downlink frequencies. The characteristics of TL1 and TL3 enhance the rectifier's operating range, thereby increasing the output dc power.

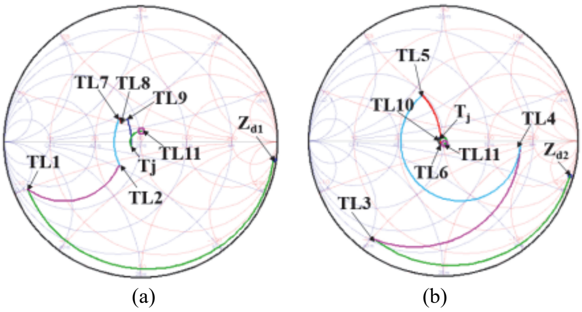

Figure 8 Design principles of matching network: (a) 0.945 GHz; (b) 1.840 GHz

The DC-pass filter is implemented using a low-impedance microstrip open-circuited line to eliminate harmonics and improve the ripple factor. The DC-pass filter is designed using a conventional open-circuit transmission line, eliminating the need for a radial stub. This design approach reduces the area required for the DC-pass filter in the layout implementation.

3.2 Performance of the Proposed Rectifier Design

The layout level simulation is carried out for the proposed rectifier design shown in the schematic of Fig. 8. The Roggers RT Duroid 3203 with a dielectric constant 3.02 and thickness 0.76 mm is used as substrate for the layout. The RT/Duroid 3203 substrate ensures stable performance in extreme conditions (–55°C to +125°C) with minimal moisture absorption, enhancing long-term reliability and reducing performance degradation. The length and width of the microstrip lines are calculated using line calculator tool in ADS software. The layout of the proposed dual-band rectifier, shown in Fig. 9, features dimensions optimized through tuning and parametric variation using ADS software.

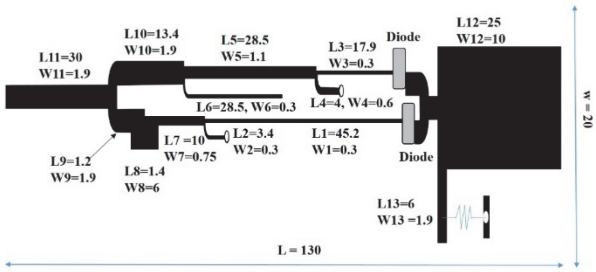

Figure 9 Layout of the proposed dual-band rectifier (all units in mm)

The input impedance of the proposed rectifier at different power levels, with a fixed load resistor of 4.7 KΩ, is shown in Fig. 10 based on layout-level simulations. A reasonable impedance match with frequency shift is observed as the power level varies from –25 dBm to –5 dBm. Among the different power levels, the impedance values are perfectly matched at –15 dBm for both bands, while at other power levels, the matching is close but accompanied by slight frequency shifts.

To validate the proposed design, fabrication is carried out and photograph of the fabricated rectifier board during the measurement process is shown in Fig. 11. The power conversion efficiency is calculated by

$$\eta = \frac{V_L^2}{R_L P_{in}} X100 \tag{1}$$

R_L is load resistance, P_{in} is input RF power and V_L is output dc voltage of the load.

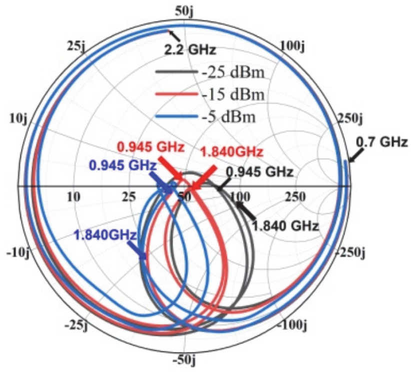

Figure 10 Input impedance of the dual band rectifier at different power levels for load resistor 4.7 KΩ

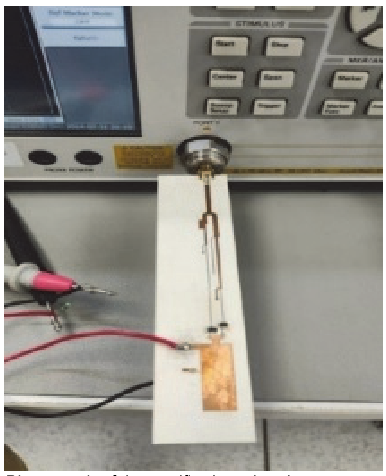

Figure 11 Photograph of the rectifier board under measurement

The simulated and measured reflection coefficients (S_{11}) in dB and PCE as a function of frequency are shown in Figs. 12 and 13, respectively. Due to fabrication errors, a frequency shift is observed in both the S_{11} and PCE measurement results for both bands. The measured maximum conversion efficiencies of 44.8% and 46.5% are achieved at 920 MHz and 1766 MHz, respectively, for a power level of –5 dBm. As shown in Tab. 2, the proposed rectifier circuit with the matching network, designed using the transmission line approach, has a bandwidth of 24-28 MHz for the GSM 900 band and 54-58 MHz for the GSM 1800 band with a 4.7 KΩ load. This results in an enhanced operating bandwidth for the rectifier, enabling maximization of the load DC power by rectifying each single tone in the intended band of harvested ambient signals. Tab. 2 also shows that the operating power level of the rectifier is improved, allowing for the maximization of the load DC power by rectifying different power levels within the intended band.

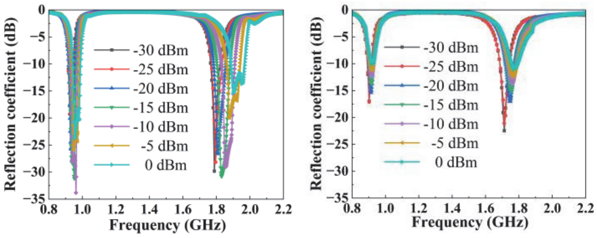

(a) (b)

Figure 12 Reflection versus frequency of the rectifier: (a) simulated; (b) measured

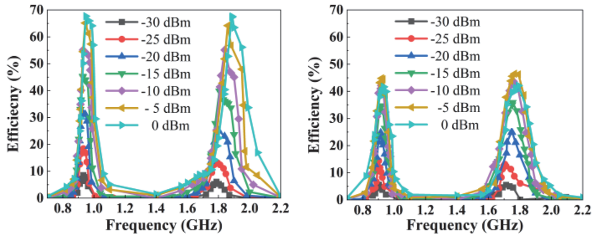

(a) (b)

Figure 13 Efficiency versus frequency of the rectifier: (a) simulated; (b) measured

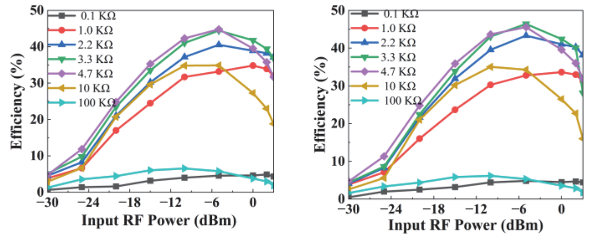

(a) (b)

Figure 14 Measured efficiency versus input power: (a) 0.915 GHz; (b) 1.75 GHz

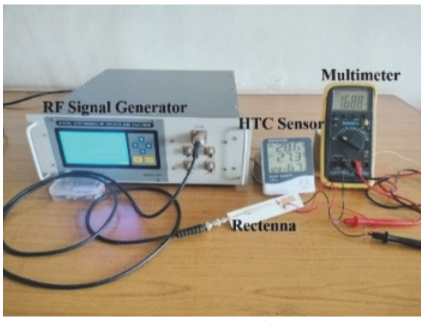

Figure 15 Photograph of experimental set-up for powering the sensor using the proposed rectifier

Table 2 Measured PCE and bandwidth of the proposed rectifier for the different power levels

Pin dBm	Freq. (MHz) S11 ≤ –10 dB GSM 900	PCE / % S11 ≤ –10 dB GSM 900	Freq. (MHz) S11 ≤ –10 dB GSM 1800	PCE / % S11 ≤ –10 dB GSM 1800
–30	892-916	4.4-5.6	1686-1738	4.6-5.5
–25	893-916	11.1-14.4	1690-1743	11.3-13.2
–20	900-928	21.3-24.8	1719-1774	21.2-24.8
–15	902-930	31.5-34.7	1724-1782	32.3-35.9
–10	905-931	39.4-42.1	1732-1789	40.3-43.7
–5	907-931	43.1-44.8	1740-1794	43.6-46.5
0	914-928	38.0-40.2	1750-1796	35.1-41.3

The measured PCE at different power levels and loads is shown in Figs. 14a and 14b for operation at 0.915 GHz and 1.75 GHz frequencies, respectively. At lower power levels, the PCE decreases due to the diode's threshold voltage, while at higher power levels (above –5 dBm), the PCE drops due to power loss in the series resistance. From Fig. 14, it is also observed that a reasonable PCE is achieved with load values ranging from 1 KΩ to 10 KΩ, due to the performance of the designed matching circuit for both frequencies. The 4.7 KΩ load is identified as the optimal load for different power levels which is suitable for various IoT low power devices. Figure 15 shows a photograph of the experimental setup used to power the sensor with the proposed rectifier. The Humidity, Temperature and Clock (HTC) sensor is powered by the fabricated rectifier circuit, with the RF input fed by the signal generator.

4 RECTENNA MEASUREMENT IN AN OUTDOOR AMBIENT ENVIRONMENT

The performance of the fabricated rectenna tested under a roof in an outdoor ambient environment is shown in Fig. 16. The distance from the nearest cell tower to the rectenna on the roof is 35 meters. For a 4.7 KΩ load, the output DC voltage ranged from 0.3 V to 0.67 V, corresponding to DC power levels of 19 µW to 96 µW in the ambient environment under the roof. In the open-circuit condition, on roof the output DC voltage ranged from 0.9 V to 1.697 V . On the ground, under open-circuit condition, the output DC voltage varied between 0.7 V and 1.6 V. When the output voltage reached approximately 1.5 V, the HTC sensor is switched ON. Hence the proposed rectenna has potential to harvest RF energy and can overcome the challenge of battery recharging and replacement in wireless sensor nodes.

Figure 16 Photograph of rectenna measurement in an outdoor environment on a roof

3 DISCUSSION OF RESULTS

The performance of the proposed rectifier design is compared with the previous researches in the Tab. 3. It is noticeable that the proposed rectifier design produces an acceptable PCE and size in comparison with the other related researches. As far as the efficiency is concerned, the proposed design achieves a PCE greater than 20% at –20 dBm, greater than 30% at –15 dBm, and greater than 40% at –10 dBm for both bands, which is comparable to the references [9] and [24] whereas in other related researches it is less. In general, the size of the dual-branch rectifier will be larger than that of the single-branch rectifier topology in order to improve the operating frequency and ambient RF power levels which in turn increases the output DC power. In this proposed design of dual branch rectifier, the size is increased which is comparable with the size of the single branch rectifier designs specified in the references [9], [24], and [25]. This shows that the size of the proposed dual branch rectifier is designed with minimum area. The maximum PCE achieved for a dual-tone input is 50% in references [9] and [24], whereas the proposed work reaches 85% in simulation due to the dual branch network. Hence it is proved that the proposed rectifier circuit effectively rectifies both bands of frequencies at ambient power levels, making it suitable for RF energy harvesting applications.

Table 3 Performance comparison of the rectifier against related works.

Ref.No.	Rectifier Topology	Diode	RF Freq. (GHz)	PCE (%) for Pin (dBm)				Size mm²
				–20	–15	–10	–5	
[4]	Single branch series	SMS 7630	0.915	15	23	33	42	19 × 21
			2.45	10	18	25	35	
[6]	Single branch series	SMS 7630	1.880	NA	18	26	32	NA
			1.980	NA	32	43	49	
[9]	Single branch series	HSMS - 2852	1.84	33	42	46	46	146 × 27
			2.14	28	42	51	55	
[18]	Single branch series	HSMS - 2860	3.5	1	8	23	44	20 × 25
			5.8	1	2	8.4	27	
[19]	Single branch series	BAT15 - 03W	0.915	5	20	35	50	21 × 19
			2.45	5	20	35	50	
[23]	Dual branch series	SMS 7630	3.5	NA	10	20	25	NA
			5.8	NA	10	20	25	
[24]	Single branch series	HSMS - 2850	1.85	25	35	43	NA	44 × 81
			2.15	28	38	47		
			2.48	19	30	38		
[25]	Single branch series	HSMS - 2852	2.45	8	23	35	47	89 × 34
			5.8	2	3	10	14	
This work	Dual branch series	HSMS - 2850	0.915	24	35	41	43	135 × 20
			1.750	24	35	43	46	

Table 4 Performance comparison of the antenna against related works

Ref. No.	RF Bands GHz	Gain dBi	Beam width	Impedance bandwidth	Size mm²
[4]	0.915	1.87	NA	NA	60 × 60
	2.45	4.18	NA		
[5]	1.8 and 2.45	7.5-10.5	NA	1.54-3.22 GHz	NA
[8]	GSM 840 GSM 1860 3G-2100 Wi-Fi	High Gain	NA	NA	150 × 150
[9]	GSM 1800	9.9-13.3	170° (HPBW)	1.8-2.2 GHz	280 × 140
	UMTS 2100	10.9-13.3	110° (HPBW)		
[10]	0.900	5.15	Omni-directional	NA	200 × 150
This work	GSM900	3-4.8	150° (HPBW)	872-1004 MHz	160 × 115
	GSM1800	2.5-3.2	230° (HPBW)	1712 -1880 MHz	

The performance of the proposed antenna design is compared with related researches in the Tab. 4. In this work, the second band is achieved by placing a half-wavelength dipole near the primary dipole, with the spacing between the driven and parasitic dipoles optimized for maximum coupling. This approach makes it easier to achieve the second band compared to the methods in [4] and [8]. Additionally, the antenna's volume is 160 × 115 × 0.76 mm³, making integration with external circuits and placement easier than in [4]. The proposed design features broaden HPBW in H-Plane for both the bands, with the second band's HPBW being twice that of the second band in reference [9]. A parasitic element in a dipole configuration is added with a minimized size compared to the design in reference [10]. From Tab. 4, it is evident that the proposed antenna achieves acceptable bandwidth, beamwidth and gain in both the bands, with compact size compared to other related researches, which proves that it is suitable for RF energy harvesting applications.

5 CONCLUSION

This study presents a compact, dual-band rectenna designed for RF energy harvesting, targeting GSM 900 and 1800 bands. The antenna, featuring a printed dipole with a parasitic dipole, achieves bandwidths of 132 MHz and 168 MHz, with measured gains between 2.5 dBi and 4.8 dBi. The rectifier circuit, utilizing transmission lines, diodes, and load resistors, demonstrates a peak power conversion efficiency (PCE) of 24.8% at –20 dBm and 44.8% at –5 dBm for a 4.7 kΩ load. The rectifier's performance is analyzed across varying power levels and load resistances, showing efficient power conversion within 25 MHz (GSM 900) and 50 MHz (GSM 1800) bandwidths, ranging from –30 dBm to –5 dBm. The transmission line-based matching network optimizes PCE, while conventional stubs minimize circuit area. In outdoor tests, the rectenna generates over 1.5 V, successfully powering an HTC sensor. This highlights its potential to energize low-power devices without batteries, especially with an integrated power management system. Future improvements may include a multiband rectenna using double-sided printed dipoles and a stacked multiband rectifier to enhance PCE and expand operational bands. Each IoT device can autonomously harvest energy through its rectenna module, while energy storage and power management enhance the reliability and scalability of large-scale, sustainable IoT networks.

6 REFERENCES

[1] Surender, D., Khan, T., Talukdar, F. A., & Antar, Y. M. (2021). Rectenna design and development strategies for wireless applications: A review. *IEEE Antennas and Propagation Magazine*, *64*(5), 16-29. https://doi.org/10.1109/map.2021.3099722

[2] Ullah, M. A., Keshavarz, R., Abolhasan, M., Lipman, J., Esselle, K. P., & Shariati, N. (2022). A review on antenna technologies for ambient RF energy harvesting and wireless power transfer: Designs, challenges and applications. *IEEE Access*, *10*, 17231-17267. https://doi.org/10.1109/ACCESS.2022.3149276

[3] Ladan, S., Ghassemi, N., Ghiotto, A., & Wu, K. (2013). Highly efficient compact rectenna for wireless energy harvesting application. *IEEE Microwave Magazine*, *14*(1), 117-122. https://doi.org/10.1109/MMM.2012.2226629

[4] Niotaki, K., Kim, S., Jeong, S., Collado, A., Georgiadis, A., & Tentzeris, M. M. (2013). A compact dual-band rectenna using slot-loaded dual band folded dipole antenna. *IEEE Antennas and Wireless Propagation Letters*, *12*, 1634-1637.

https://doi.org/10.1109/LAWP.2013.2294200

[5] Chandravanshi, S., Katare, K. K., & Akhtar, M. J. (2018). Design of dual band compact wireless energy harvesting circuit for GSM and WLAN band. *2018 IEEE MTT-S International Microwave and RF Conference*, 1-4. https://doi.org/10.1109/IMaRC.2018.8877332

[6] Khemar, A., Kacha, A., Takhedmit, H., & Abib, G. (2018). Design and experiments of a dual-band rectenna for ambient RF energy harvesting in urban environments. *IET Microwaves, Antennas & Propagation*, *12*(1), 49-55. https://doi.org/10.1049/iet-map.2016.1040

[7] Adam, I., Yasin, M. N. M., Rahim, H. A., Soh, P. J., & Abdulmalek, M. F. (2018). A compact dual-band rectenna for ambient RF energy harvesting. *Microwave and Optical Technology Letters*, *60*(11), 2740-2748. https://doi.org/10.1002/mop.31475

[8] Vu, H. S., Nguyen, N., Ha-Van, N., Seo, C., & Le, M. T. (2020). Multiband ambient RF energy harvesting for autonomous IoT devices. *IEEE Microwave and Wireless Components Letters*, *30*(12), 1189-1192. https://doi.org/10.1109/LMWC.2020.3029869

[9] Ganesan, R., Panchavarnam, M. V., & Thangaiyan, J. (2023). Split ring resonator inspired dual-band monopole antenna for ISM, WLAN, WIFI, and WiMAX application. *Tehnički vjesnik/Technical Gazette*, *30*(5), 1533-1538. https://doi.org/10.17559/TV-20230210000344

[10] Sun, H., Guo, Y. X., He, M., & Zhong, Z. (2013). A dual-band rectenna using broadband Yagi antenna array for ambient RF power harvesting. *IEEE Antennas and Wireless Propagation Letters*, *12*, 918-921. https://doi.org/10.1109/LAWP.2013.2272873

[11] Nakashima, N. & Sumiyoshi, T. (2024). A prototype of a 900 MHz band integrated rectenna by using a planar monopole antenna with feeder. *Radio Science*, *59*(8), 1-2. https://doi.org/10.1029/2024RS008022

[12] Wheeler, H. A. (1965). Transmission-line properties of parallel strips separated by a dielectric sheet. *IEEE Transactions on Microwave Theory and Techniques*, *13*(2), 172-185. https://doi.org/10.1109/TMTT.1965.1125962

[13] Armagan, O. & Kahriman, M. (2022). The effect of the co-planar structure on HPBW and the directional gain at the square patch antenna around ISM 2450 MHz. *Tehnički vjesnik/Technical Gazette*, *29*(4), 1120-1125. https://doi.org/10.17559/TV-20190423010908

[14] Floc'h, J. M. & Rmili, H. (2006). Design of multiband printed dipole antennas using parasitic elements. *Microwave and Optical Technology Letters*, *48*(8), 1639-1645. https://doi.org/10.1002/mop.21714

[15] Zheng, G., Kishk, A. A., Glisson, A. W., & Yakovlev, A. B. (2004). Simplified feed for modified printed Yagi antenna. *Electronics Letters*, *40*(8), 464-466. https://doi.org/10.1049/el:20040348

[16] Chang, K., Kim, H., & Yoon, Y. J. (2005). A triple-band printed dipole antenna using parasitic elements. *Microwave and Optical Technology Letters*, *47*(3), 221-223. https://doi.org/10.1002/mop.21129

[17] Chen, J. X., Chin, C. H., & Xue, Q. (2007). Double-sided parallel-strip line with an inserted conductor plane and its applications. *IEEE Transactions on Microwave Theory and Techniques*, *55*(9), 1899-1904. https://doi.org/10.1109/TMTT.2007.904055

[18] Kim, S. G. & Chang, K. (2004). Ultra-wide-band transitions and new microwave components using double-sided parallel-strip lines. *IEEE Transactions on Microwave Theory and Techniques*, *52*(9), 2148-2152. https://doi.org/10.1109/TMTT.2004.834165

[19] Li, Z., Zhang, J. W., Wang, Y. C., He, D. P., & Zhang, C. (2023). Two-port five-band rectenna for ultralow ambient rf energy harvesting. *IEEE Antennas and Wireless Propagation Letters*, *22*(8), 1972-1976. https://doi.org/10.1109/LAWP.2023.3270935

[20] Wang, C., Zhang, J., Bai, S., Chang, D., & Duan, L. (2023). A multiband compact flexible energy collector for wearable or portable IoT devices. *IEEE Antennas and Wireless Propagation Letters*, *22*(5), 1164-1168. https://doi.org/10.1109/LAWP.2023.3235918

[21] Halimi, M. A., Khan, T., Koul, S. K., & Rengarajan, S. R. (2022). A dual-band rectifier using half-wave transmission line matching for 5G and Wi-Fi bands RFEH/MPT applications. *IEEE Microwave and Wireless Technology Letters*, *33*(1), 74-77. https://doi.org/10.1109/LMWC.2022.3197590

[22] Li, S., Cheng, F., Gu, C., Yu, S., & Huang, K. (2021). Efficient dual-band rectifier using stepped impedance stub matching network for wireless energy harvesting. *IEEE Microwave and Wireless Components Letters*, *31*(7), 921-924. https://doi.org/10.1109/LMWC.2021.3078546

[23] Palazzi, V., Hester, J., Bito, J., Alimenti, F., Kalialakis, C., Collado, A., Mezzanotte, P., Georgiadis, A., Roselli, L., & Tentzeris, M. M. (2017). A novel ultra-lightweight multiband rectenna on paper for RF energy harvesting in the next generation LTE bands. *IEEE Transactions on Microwave Theory and Techniques*, *66*(1), 366-379. https://doi.org/10.1109/TMTT.2017.2721399

[24] Song, C., Huang, Y., Carter, P., Zhou, J., Yuan, S., Xu, Q., & Kod, M. (2016). A novel six-band dual CP rectenna using improved impedance matching technique for ambient RF energy harvesting. *IEEE Transactions on Antennas and Propagation*, *64*(7), 3160-3171. https://doi.org/10.1109/TAP.2016.2565697

[25] Marian, V., Allard, B., Vollaire, C., & Verdier, J. (2012). Strategy for microwave energy harvesting from ambient field or a feeding source. *IEEE Transactions on Power Electronics*, *27*(11), 4481-4491. https://doi.org/10.1109/TPEL.2012.2185249

[26] Derbal, M. C. & Nedil, M. (2020). A high gain dual band rectenna for RF energy harvesting applications. *Progress in Electromagnetics Research Letters*, *90*, 29-36. https://doi.org/10.2528/PIERL19122604

[27] Shen, S., Zhang, Y., Chiu, C. Y., & Murch, R. (2019). A triple-band high-gain multi beam ambient RF energy harvesting system utilizing hybrid combining. *IEEE Transactions on Industrial Electronics*, *67*(11), 9215-9226. https://doi.org/10.1109/TIE.2019.2952819

[28] Jansirani, G. & Gandhi Raj, R. (2024). Miniaturised Wide and Dual band Reconfigurable Antenna on-demand for Portable Wireless Devices. *Tehnicki vjesnik/Technical Gazette*, *31*(6), 2022-2027. https://doi.org/10.17559/TV-20240122001282

[29] Kaviarasu, K. & Ganesh, V. (2015). Design and simulation of a 900 MHz rectifier for Rectenna application. *2015 International Conference on Communications and Signal Processing (ICCSP)*, 0754-0756. https://doi.org/10.1109/ICCSP.2015.7322592

Contact information:

V. GANESH, Assistant Professor
(Corresponding author)
Department of Electronics and Communication Engineering,
Sri Ramakrishna Institute of Technology,
Coimbatore, Tamil Nadu, India
E-mail: ganeshperumal.ece@outlook.com

Dr. H. MANGALAM, Professor
Department of Electronics and Communication Engineering,
Sri Ramakrishna Engineering College,
Coimbatore, Tamil Nadu, India
E-mail: hmangalam2@gmail.com